한국소성가공학회 2004년도 춘계학술대회 논문집 pp.214~220

튜브 하이드로포밍 공정의 성형한계 해석

김진* · 박춘달** · 김영석*** · 이재용*

Analysis of forming limit in tube hydroforming process

J. Kim, C. D. Park, Y. S. Kim and J. Y. Lee

Abstract

The automotive industry has recently shown a growing interest in tube hydroforming. Even though many structural parts in automotives have been produced from the cylindrical tubes, many failures - wrinkling, buckling, folding back, bursting and so on - are frequently experienced during the tube hydroforming process under improper forming conditions. In this paper, analytical studies are performed to determine the forming limits for the tube hydroforming process and demonstrate how the loading path influences the forming limit. The theoretical results for the forming limits of the wrinkling and bursting are then compared with the experimental results for an aluminum tube.

Key Words : Tube Hydroforming, Forming Limit, Bursting, Wrinkling

1. Introduction

Tube hydroforming is a relatively new technology that is currently enjoying increasingly widespread industrial application. This technology has already been widely utilized in fields such as the pipe fitting industry and bicycle industry because of its suitability for manufacturing light and high-rigidity parts. Recently, the use of tube forming technology in the manufacture of automobile parts has increased, where many automotive part manufacturers have started to make the hollow parts of structure components using tube hydroforming to achieve a weight reduction, improve the strength reliability of the products, and reduce the process numbers and cost. [1-4]

The forming principle behind the hydroforming process involves a starting tube being aligned to the internal surface of a tool that encloses the tube through the combined action of mechanical loading and hydrostatic internal pressure [5-7]. The implementation of this principle leads to highly complex process sequence with a large number of parameters related to the tube, the tool and the process working together to achieve a successful forming products. . There is always a danger of premature work piece failures – buckling, bursting, wrinkling and so on - because of incorrectly adjusted process parameters or tube dimensions and shapes that do not correspond to the required design of the part. The occurrence of these forming failures represents the forming limit of the tubes [8,9]. The selective control of the tube forming process and the availability of a forming machine that is commensurate with the requirements of the process are thus of key

* 경북대학교 기계공학부 대학원
** 현대자동차
*** 경북대학교 기계공학부
* 경북대학교 기계공학부 대학원

importance for the successful application of this technology [10-14].

In order to obtain safely formed products without such forming failures, the loading path between the axial feeding and the internal pressure must be controlled simultaneously to improve tube formability.

In this paper we analytically investigate the forming limits for the tube hydroforming process, especially bursting and wrinkling failures, and the predicted results are compared with the experimental results for an aluminum tube [5]. Due to the insufficiently of Hill's anisotropy yield criterion[15] to describe the plastic behavior of aluminum tube material having R<1.0, we adopted Hosford yield criterion[16] in this study.

2. Analytical Study

2.1 Theoretical background

A tube is modeled as a thin-walled axisymmetrical shell in which the directions of the principal stresses σ_l, σ_θ and σ_t at any point are the axial, circumferential and thickness directions, respectively. It is assumed that σ_t is negligible and that the principal axes of the strain increments $d\varepsilon_l$, $d\varepsilon_\theta$ and $d\varepsilon_t$ coincide with the principal stress axes.

Here, Hosford's yield criterion for anisotropic material [16] is employed to describe the plastic deformation behavior of the tube subjected to hydrostatic pressure. Then, the equivalent stress can be written as follows:

$$|\sigma_l|^a + |\sigma_\theta|^a + R|\sigma_l - \sigma_\theta|^a = (R+1)\bar{\sigma}^a \qquad (1)$$

The corresponding flow rules are

$$\frac{d\varepsilon_l}{|\sigma_l|^{a-1} + R|\sigma_l - \sigma_\theta|^{a-1}} = \frac{d\varepsilon_\theta}{|\sigma_\theta|^{a-1} - R|\sigma_l - \sigma_\theta|^{a-1}} = \frac{d\varepsilon_l}{-(|\sigma_l|^{a-1} + R|\sigma_\theta|^{a-1})} = \frac{d\bar{\varepsilon}}{(1+R)\bar{\sigma}^{a-1}} \qquad (2)$$

Here, R is an anisotropic parameter. And the exponent a is greater than 2. With $a=2$, this criterion simplifies to Hill's anisotropic yield criterion[15]. Kim, et al.[17] evaluated the formability of tube under hydroforming for anisotropic material using the Hill's criterion. They showed that the bursting limit of tube overestimated the experimental data[5] by adopting Hill's anisotropic yield criterion. However, the crystallographic calculations are much better approximated by $a=6$ for BCC metals and $a=8$ for FCC metals.

Also, the work hardening characteristics of the material is assumed to follow the power law,

$$\bar{\sigma} = K\bar{\varepsilon}^n \qquad (3)$$

where, K is the strength coefficient and n is the work hardening exponent. From the volume constancy,

$$d\varepsilon_l + d\varepsilon_\theta + d\varepsilon_t = 0 \qquad (4)$$

Assuming that principal stresses maintain constant their ratios and directions, the ratios of the strain increments will be fixed, such that

$$\alpha = \frac{\sigma_l}{\sigma_\theta}, \quad \gamma = \frac{d\varepsilon_l}{d\varepsilon_\theta} = \frac{|\alpha|^{a-1} + R|\alpha-1|^{a-1}}{1 - R|\alpha-1|^{a-1}} \qquad (5)$$

From Eq. (1) and Eq. (2), hoop directional stress and strain are expressed as follows :

$$\sigma_\theta = \left(\frac{R+1}{1+|\alpha|^{a-1} + R|\alpha-1|^{a-1}}\right)^{1/a} \bar{\sigma} \qquad (6)$$

$$\varepsilon_\theta = \frac{\bar{\varepsilon}}{(1+R)\bar{\sigma}^{a-1}} |\sigma_\theta|^{a-1} (1 - R|\alpha-1|)^{a-1} \qquad (7)$$

Also, substituting Eq. (6) into Eq. (7)

$$\varepsilon_\theta = \frac{1 - R|\alpha-1|^{a-1}}{(1+R)^{1/a}(1+|\alpha|^a + R|\alpha-1|^a)^{\frac{a-1}{a}}} \bar{\varepsilon} \qquad (8)$$

Substituting the hoop directional stress $\sigma_\theta = \frac{pr}{t} > 0$ into Eq. (7), the following relationship between internal pressure and strain component is obtained.

$$p = \frac{t}{r}\frac{\bar{\sigma}}{\bar{\varepsilon}^{\frac{1}{a-1}}}\left(\frac{1+R}{1-R|\alpha-1|^{a-1}}\varepsilon_\theta\right)^{\frac{1}{a-1}} = \frac{t}{r}K\bar{\varepsilon}^{n-\frac{1}{a-1}}\left(\frac{1+R}{1-R|\alpha-1|^{a-1}}\varepsilon_\theta\right)^{\frac{1}{a-1}} \qquad (9)$$

where p is the internal pressure in the tube. t is the tube wall thickness at any instant and r is the instantaneous tube radius measured perpendicularly to the axis of tube during bulging defined as follows :

$$t = t_0 \exp(\varepsilon_t) = t_0 \exp\{-(\gamma + 1)\varepsilon_\theta\}$$
$$r = r_0 \exp(\varepsilon_\theta) \tag{10}$$

Consider the tube is subject to the combination action of the internal pressure p and axial compressive forces F as in Fig. 1. For an element at the middle of this tube, the following equilibrium equations can be written.

$$\sigma_\theta = \frac{pr}{t} \tag{11}$$

$$\sigma_l = \frac{pr}{2t} - \frac{F}{2\pi rt} \tag{12}$$

Assume that the tube hydroforming tool has the shape shown in Fig. 1.

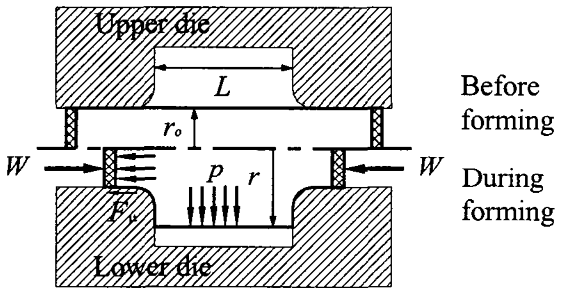

Fig. 1 Principle of tube hydroforming (original tube shape and intermediate shape of tube

Then, the forming force can be defined as $F = W - F_{sealing} - F_{friction}$. The sealing force applied at both ends of the tube can be written as $F_{sealing} = p\pi r_0^2$. In this study, we assume there is no friction force ($\mu = 0$).

2.2 Necking criterion of tube during the bulging process

Diffused necking in the circumferential direction can occur at maximum internal pressure. The critical stresses and strains in the tube wall at this instant can be derived as follows [18-19]:

$$dp = d\left(\frac{\sigma_\theta t}{r}\right) = 0 \tag{13}$$

That is,

$$\frac{d\sigma_\theta}{\sigma_\theta} = (\gamma + 2) d\varepsilon_\theta \tag{14}$$

From Eq.(6), Eq.(14) is also written as follows:

$$\frac{d\bar{\sigma}}{\bar{\sigma}} = (\gamma + 2) d\varepsilon_\theta \tag{15}$$

Hence, substituting Eq. (8) into Eq. (15)

$$\frac{d\bar{\sigma}}{\bar{\sigma}} = (\gamma + 2) \frac{1 - R|\alpha - 1|^{a-1}}{(1+R)^{1/a}(1 + |\alpha|^a + R|\alpha - 1|^a)^{\frac{a-1}{a}}} d\bar{\varepsilon} \tag{16}$$

or

$$\frac{d\bar{\sigma}}{d\bar{\varepsilon}} = (\gamma + 2) \frac{1 - R|\alpha - 1|^{a-1}}{(1+R)^{1/a}(1 + |\alpha|^a + R|\alpha - 1|^a)^{\frac{a-1}{a}}} \bar{\sigma} \tag{17}$$

Using the stress-strain relationship of Eq. (3), above equation yields the following effective strain at instability:

$$\bar{\varepsilon}_{\max} = \frac{n}{(\gamma + 2)} \frac{(1+R)^{1/a}(1 + |\alpha|^a + R|\alpha - 1|^a)^{\frac{a-1}{a}}}{1 - R|\alpha - 1|^{a-1}} \tag{18}$$

It is very interesting to note that the effective strain to diffuse necking occurrence does not depend on the loading path since there is no integration over the strain path in its derivation. Substituting Eq. (18) into Eq. (8), the following relationship is derived

$$\varepsilon_{\theta,\max} = \frac{n}{\gamma + 2} \tag{19}$$

or

$$\varepsilon_{l,\max} + 2\varepsilon_{\theta,\max} = n \tag{20}$$

From the volume constancy, the maximum thickness strain at instability is given by

$$\varepsilon_t = -\frac{\gamma + 1}{\gamma + 2} n \tag{21}$$

If we preserve the value of strain increment ratio γ at -1, the thickness strain is zero from Eq. (21). This means that the wall thickness remains constant during tube hydroforming operation. From Eq. (21) we can conclude that very large bulging forming of the tube is possible without thickness reduction provided a sufficiently large axial compression balanced with internal pressure is applied.

In this paper, as a criterion of instability occurrence, we adopt the following experimental equation with FLC_0 of the forming limit curve (FLC), which was determined from the tube bulging test [8]:

$$\varepsilon_{l,\max} + 2\varepsilon_{\theta,\max} = \ln(1 + 0.01FLC_0) \tag{22}$$

Using this relation and Eq. (9), we can obtain the following relationship between the bursting pressure and the strain component:

$$p_{cr} = \frac{t}{r}\frac{\bar{\sigma}}{\varepsilon_{\max}^{-\frac{1}{a-1}}}\left(\frac{1+R}{1-R|\alpha-1|^{a-1}}\varepsilon_{\theta,\max}\right)^{\frac{1}{a-1}} = \frac{t}{r}K\bar{\varepsilon}_{\max}^{n-\frac{1}{a-1}}\left(\frac{1+R}{1-R|\alpha-1|^{a-1}}\varepsilon_{\theta,\max}\right)^{\frac{1}{a-1}} \tag{23}$$

2.3 Forming limit of wrinkling during the bulging process

A second possible mode of failure is a wrinkling of the tube due to excessively high axial compressive stress. Although there are several modes of wrinkling, the most likely mode is the formation of an axisymmetric wrinkle of the tube. The critical wrinkling stress is obtained as follows:

If the cylindrical tube is loaded under the combination action of axial load and internal pressure, the following differential equation for symmetrical deflection of a cylindrical shell can be used in calculating the critical load for wrinkling occurrence.

$$D\frac{d^4 w}{dw^4} - N_l\frac{d^2 w}{dw^2} + \frac{E_s t_o}{r_0^2}w = p \tag{24}$$

where N_l is a normal force per unit distance in the shell ($N_l = \sigma_l t_0$) and is considered positive when it is under compression. w is the displacement in the thickness direction. D is the flexural rigidity of the shell defined as follows:

$$D = \frac{Et_0^3}{12(1-\nu)} \tag{25}$$

In addition, plastic deformation may be defined as follows:

$$D = \frac{Et_0^3}{12(1-\nu)} = \frac{E_r t_0^3}{9} \tag{26}$$

Here E_r is a reduced modulus of elasticity and is defined as follows:

$$E_r = \frac{4EE_t}{\left(\sqrt{E}+\sqrt{E_t}\right)^2} \tag{27}$$

where E is an elastic modulus and E_t is a tangent modulus. Both moduli are defined as

$E = \bar{\sigma}/\bar{\varepsilon} = K\bar{\varepsilon}^{n-1}$ and $E_t = \overline{d\sigma}/\overline{d\varepsilon} = nK\bar{\varepsilon}^{n-1}$.

Radial displacement w is assumed by the following equation for axisymmetric wrinkling formation:

$$w = -A\sin\frac{m\pi x}{l} \tag{28}$$

where l is the length of the cylinder and m is the number of a half wave length.

Substituting Eq. (28) to Eq. (24) and equating the coefficient of $\sin(m\pi x)$ to zero, we obtain the equation of the critical wrinkling stress.

$$\sigma_{cr} = \frac{N_{cr}}{t_0} = D\left(\frac{m^2\pi^2}{t_0 l^2} + \frac{E}{r_0^2 D}\frac{l^2}{m^2\pi^2}\right) \tag{29}$$

Assuming that there are many waves formed along the length of the cylinder during wrinkling formation and also considering σ_{cr} as a continuous function of $m\pi/l$, the above equation can be simplified as follow:

$$\sigma_{cr} = \frac{2}{r_0 t_0}\sqrt{EDt_0} \tag{30}$$

and wrinkling occurs at

$$\frac{m\pi}{l} = \sqrt[4]{\frac{Et_0}{r_0 D}} \tag{31}$$

Therefore Eq. (30) gives the limit of wrinkling occurrence of the cylindrical tube under the combination action of axial load and internal pressure. However this equation only predicts that the wrinkling of the tube occurs along the full length of the tube and that the amplitude of the wave is constant along the full length of the tube. In practice, however, this situation rarely occurs since the major part of the ends of the tube specimen is constrained by the sealing die compressing both ends of the tube. The real phenomenon shows wrinkling is almost confined near both ends of the tube and the amplitude of the wave decreases towards the center of the tube.

Substituting Eq. (25) and Eq. (26) into Eq. (30) the critical stress at wrinkling occurrence is expressed as follows:

$$\sigma_{cr} = \frac{Et_0}{r_0\sqrt{3(1-\nu^2)}} \tag{32}$$

$$\sigma_{cr} = \frac{4Et_0}{3r_0\left(1+\sqrt{\frac{E}{E_t}}\right)} \tag{33}$$

Equations (32) and (33) yield the critical stresses at wrinkling occurrence for elastic and plastic deformation regions of the tube, respectively.

3. Results and Discussion

The tube considered in this study is aluminum used in the experiment [5]. The mechanical properties are shown in Table 1. The parameters of the aluminum tube are as follows: the tube length of the expansion zone, $L = 100mm$; the average initial tube radius, $r_o = 24.5mm$; and the initial tube thickness, $t_o = 1mm$.

Table 1 Mechanical properties of aluminum

$K(kg_f/mm^2)$	15
n	0.24
$TS(kg_f/mm^2)$	8.8
$El(\%)$	35.9
R	0.75

where, $\bar{\sigma} = K\bar{\varepsilon}^n$

Figure 2 shows the relationship between the forming pressure and the forming radius obtained by Eq. (9) in the case of various loading paths, plane strain ($\gamma = 0$), pure shear ($\gamma = -1$) and uniaxial tension ($\gamma = -0.5$).

The forming pressure decreases and becomes slack after a sudden increase with each drawing mode according to an increase in the forming radius. After reaching the maximum forming pressure, the pressure at the plane strain forming mode drastically decreases with the forming radius. Also, as the forming mode changes from $\gamma = 0$ to $\gamma = -0.5$ and $\gamma = -1$, the forming pressures become generally lower and the forming radii with the maximum forming pressure increase. The maximum pressure is highest at $\gamma = 0$ while lowest at $\gamma = -1$. However, for the forming mode of $\gamma = -1$, the forming radius denoting the maximum pressure is not clear, compared with the other drawing modes. The maximum expansion of the tube occurs at the forming mode $\gamma = -1$. This means that the tube forming radius highly increases as high compression is actively applied at the both ends of the tube.

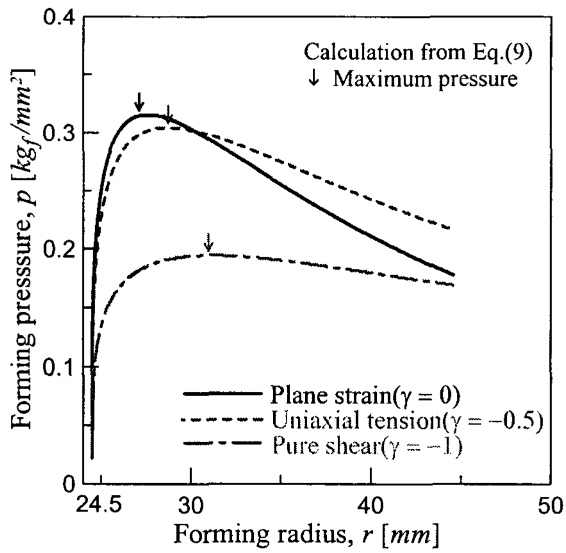

Fig. 2 Relationship between forming pressure and forming radius along each forming mode

Figure 3 shows the relationship between the bursting pressure and the axial strain, as determined by Eq. (23), with the occurrence of a neck. The maximum value of the bursting pressure is near the plane strain forming mode ($\varepsilon_l = 0$). The value, thereafter, decreases with an increase in the axial compressive strain. From the experimental results with a Cu tube by Fuchizawa [5], it was reported that the strain state is almost sustained in a plane strain state for the case of the initial length and diameter ratio, $L/D \geq 2$. Therefore, it is important to preserve $L/D \geq 2$ to estimate the lowest value of the forming limit for the maximum allowable expansion of a tube under tube hydroforming process like the FLDo value in the forming limit diagram of sheet metal.

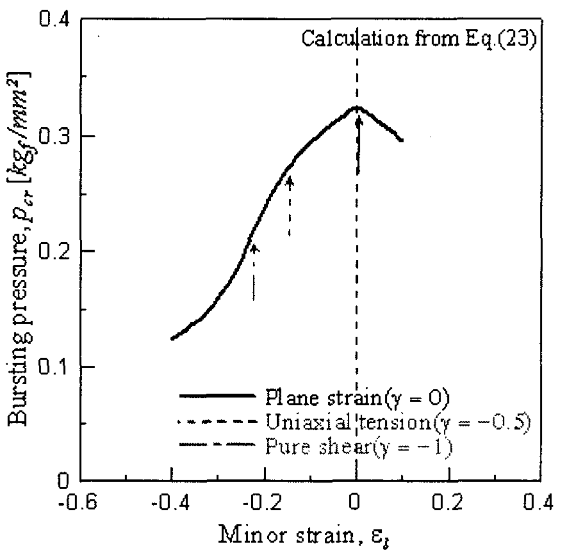

Fig. 3 Relationship between bursting and minor strain

Figure 4 shows a comparison between the theoretical analysis and the experimental results [5] for the occurrences of wrinkling and bursting. The yielding limit of the tube material is predicted from Eqs. (9) and (13). The bursting limit and wrinkling limit are analyzed on the basis of Eqs. (23) and (33) and compared with the experimental results for an aluminum tube during the tube hydroforming process. The wrinkling limit obtained from the theoretical analysis is in good agreement with the experimental results. As the stress ratio has a lower value, the axial compressive stress also has a lower value. Comparing the occurrences of the bursting limit shows that the theoretical analysis slightly overestimates the experimental results. However, the theoretical result by adopting Hosford yield criterion on this study largely improved compared with that of Hill yield criterion[18]. Furthermore, it must be also recognized that the wrinkling limit should be considered first when the forming mode has a negative stress ratio. Conversely, the bursting limit should be considered first when the forming process proceeds with a positive stress ratio during tube hydroforming.

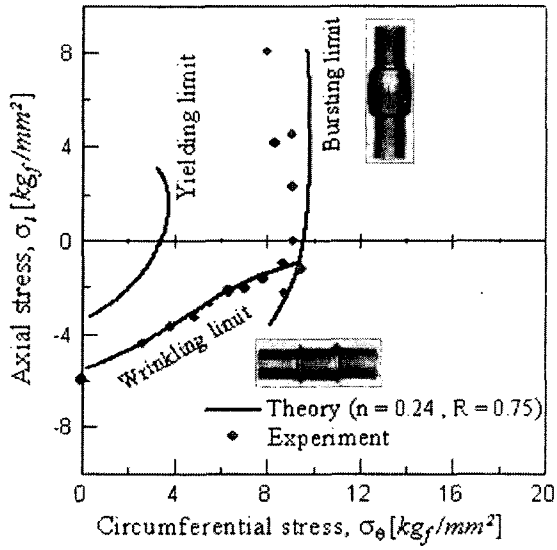

Fig. 4 Comparison between theoretical analysis and the experimental results[5] for the occurrences of bursting and wrinkling

4. Conclusions

This paper theoretically investigated the forming limits for failure occurrence, such as bursting and wrinkling, under the internal pressure and axial compression in the tube hydroformng process. The results were then compared with the experimental results. The output can be summarized as follows.

(1) The maximum expansion of the circumferential

direction was obtained with the pure shear forming mode ($\gamma = -1$).

(2) The maximum value for the bursting pressure is with the near plane strain forming mode ($\gamma = 0$).

(3) The wrinkling limit obtained from the theoretical analysis is in good agreement with the experimental results. However, the theoretical analysis slightly overestimated the experimental results for the occurrences of bursting.

Acknowledgements

This work was sponsored by Hwashin Company at Brain Korea 21 project, Kyungpook National University.

References

(1) Dohmann, F., Hartl., Ch., Tube hydroforming - research and practical application, J. Mat. Proc.Tech., 1997; 71; pp.174-186.

(2) Ahmetoglu, M, Sutter, K., Altan, T., Tube hydroforming - current research, applications and need for training, J. Japanese Soc. Tech. Plasticity, 1998; 39(453); pp.43-48.

(3) Hashmi, M. S. J., Radial thickness distribution around a hydraulically bulge formed annealed copper T-joint: experiment and theoretical predictions, 22nd Int. M.T.D.R. Conf., 1981; pp.507-516

(4) Lenz, F.J., Hoffmann, D., Application of hydroforming for body-in-white., IBEC 97 Body Assembly & Manufacturing, 1997; pp.120-128.

(5) C. Back, M. Miyagawa, The plastic deformation and strength of circular cylindrical shells under internal pressure and/or axial force(1st report, experiment), Trans. Jpn. Soc. Mech. Eng. 32 (235) (1966) 447-456

(6) Thiruvarudchelvan, S., Lua, A. C., Bulge forming of tubes with axial compressive force proportional to the hydraulic pressure, Int. J. Mater. Shaping Tech., 1991; 9; pp.133-142

(7) Tirosh,J., Neuberger,A., Shirizly,A., On tube expansion by internal fluid pressure with additional compressive stress, Int. J. Mech. Sci., 1996; 38; pp.839-851

(8) Park,J.S., Kim, J.H., Park, C.D., Kim, Y.S., Development of hydroforming simulator for thin walled tube, Proc. Japanese Soc. Tech. Plasticity, 1999; pp.235-236

(9) Stout, M. G., Hecker, S. S., Role of geometry in plastic instability and fracture of tube and sheets, Mechanics of Materials, 1983; 2; pp.23-31

(10) Miyagawa, M., Oshima, K., Plastic buckling of cylinder shells under axial compression and external pressure, J.Japanese Soc. Tech. Plasticity, 1968; 9(85); pp.80-85

(11) Mori, S., Manabe, K., Nishimura, H., Development of hydraulic bulge forming simulator for thin walled tubes and its application to experiment of loading path control, J. Japanese Soc. Tech. Plasticity, 1988; 29(325); pp.131-138

(12) Hashmi, M. S. J., Forming of tubular components from straight tubing using combined axial load and internal pressure: theory and experiment, Proc. Int. Conf. On Dev. On Drawing of Metals Society, 1983; pp.146-155

(13) Ahmed, M., Hashmi,M. S. J., Estimation of machine parameters for hydraulic bulge forming of tubular components, J. Mater. Proc. Tech., 1997; 64; pp.9-23

(14) Kim, Y.S., Cho, H.S., Park, C.D., Kim, Y.S. and Jo, Y.J., Evaluation of tube hydroformability, Korean Society for Technology of Plasticity, 2000; 9(6); pp.604-614

(15) Hill. R., The Mathematical Theory of Plasticity, Oxford University Press, 1950, London

(16) Hosford, W.F., On yield loci of anisotropic cubic metals, Proc. 7th North Am. Metalworking Conf., SME, Dearborn, MI, USA, 1979; pp.191-200.

(17) Mellor, P.B., Tensile instability in thin-walled tubes, J.Mech.Engrg.Sci., 1962; 4, pp.251-257

(18) Kim, S.T., Kim, Y.S., Analytical study for tube hydroforming, J. Mater. Process. Technol., 2002; 128; pp.232-239

(19) Kim,Y.S., Theory of engineering plasticity, Sigma Press, 2001,Seoul, Korea.